8

Advanced Trends in Design of Slip Displacement Sensors for Intelligent Robots

Y. P. Kondratenko[1] and V. Y. Kondratenko[2]

[1]Petro Mohyla Black Sea State University, Ukraine
[2]University of Colorado Denver, USA
Corresponding author: Y. P. Kondratenko <y_kondrat2002@yahoo.com>

Abstract

The paper discusses advanced trends in design of modern tactile sensors and sensor systems for intelligent robots. The main focus is the detection of slip displacement signals corresponding to object slippage between the fingers of the robot's gripper.

It provides information on three approaches for using slip displacement signals, in particular, for the correction of the clamping force, the identification of manipulated object mass and the correction of the robot control algorithm. The study presents the analysis of different methods for the detection of slip displacement signals, as well as new sensor schemes, mathematical models and correction methods. Special attention is paid to investigations of sensors developed by the authors with capacitive, magnetic sensitive elements and automatic adjustment of clamping force. The new research results on the determination of object slippage direction based on multi-component capacity sensors are under consideration when the robot's gripper collides with the manipulated object.

Keywords: slip displacement, tactile sensor, gripper, intelligent robot, model, information processing.

Advances in Intelligent Robotics and Collaborative Automation, 167–192.

8.1 Introduction

Updated intelligent robots pose high-dynamic characteristics and effectively function under a particular set of conditions. The robot control problem is more complex in uncertain environments, as robots are usually lacking flexibility. Supplying robots with effective sensor systems provides essential extensions of their functional and technological feasibility [11]. For example, a robot may often encounter a problem of gripping and holding *i* object doing manipulation processes with the required clamping force F_i^r avoiding its deformation or mechanical injury, $i = 1...n$. To successfully solve the current tasks, the robots should possess the capability to recognize the objects by means of their own sensory systems. Besides, in some cases, the main parameter due to which robot can distinguish objects of the same geometric shape is their mass $m_i (i = 1...n)$. The robot sensor system should identify the mass m_i of each *i*-th manipulated object in order to identify a class (set) an object refers to.

The sensor system should develop the required clamping force F_i^r corresponding to mass value m_i, as $F_i^r = f\ (m_i)$. Such current data may be applied when the robot functions in dynamic or random environments. For example, in a case when the robot should identify unknown parameters for any type of object and location in robot's working zone. The visual sensor system may not always be utilized, in particular, in poor vision conditions. Furthermore, in cases when the robot manipulates with an object of variable mass $m_i(t)$, its sensor system should provide the appropriate change of clamping force value $F_i^r\ (t) = f\ [m_i\ (t)]$ for the gripper fingers. This information can also be used for the robot control algorithm correction, since the mass of the robot arm's last component and its summary inertia moment vary.

8.2 Analysis of Robot Task Solving Based on Slip Displacement Signals Detection

One of the current approaches to solving the mass m_i identification problem of grasped objects and producing the required clamping force F_i^r is in the development of tactile sensor systems based on object slippage registration [1, 11, 17, 18, 20, 22] while slipping between the gripper fingers (Figure 8.1).

As usual, the slippage signal detection in robotic systems is accomplished either in the trial motion or in the regime of continuous lifting of the robot arm. In some cases, during the process of trial motions, it is necessary to make a series of trial motions (Figure 8.2) for creating the required clamping forces

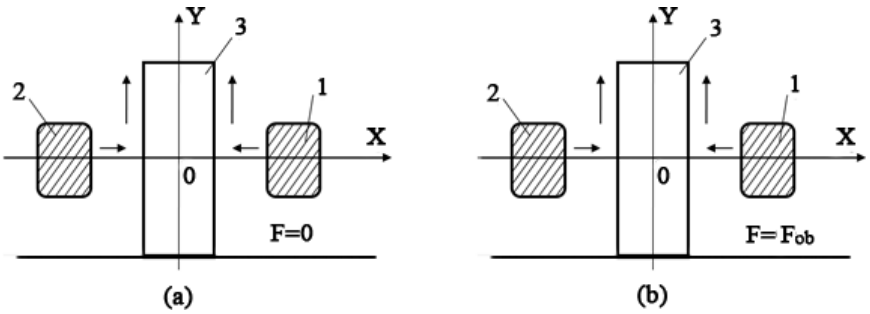

Figure 8.1 Grasping and lifting an object with the robot's arm: Initial positions of the gripper fingers (1,2) and object (3) (a); Creating the required clamping force F_{ob} by the gripper fingers during object slippage in the lifting process (b).

F_{ob} or $F_{ie} = kF_{ob}$, where k is a coefficient which impacts the reliability of the object motion (by the robot arm) in the realisation of the required path, $k > 1$.

According to Figure 8.2, the robot creates a minimal value of clamping force F_{min} in time moment t_1. Then step by step robot lifts an object vertical distance Δl and the robot gripper increases the clamping force ($F(t_1) + \Delta F$) if a slip displacement signal appears. The grasping surface of the object is limited by value l_{max}. The first series of trial motions is finished in time moment t_2, when $l = l_{max}$ (Figure 8.1(b)). After that, the robot decompresses the fingers ($t_2...t_3$), moves the gripper ($t_3...t_4$) to the initial position (Figure 8.1(a)) and creates ($t_4...t_5$) the initial value of the clamping force $F(t_5) = F(t_2) + \Delta F = F_1$ for the beginning of a second stage or second series of trial motions.

Some sensor systems based on the slip displacement sensors were considered in [24, 25], but random robot environments very often requires the development of new robot sensors and sensor systems for increasing the speed of operations, the growth of positioning accuracy or the desired path-following precision.

Thus, the task of the registration of slippage signals between the robot fingers for manipulated objects is connected with: a) the necessity of the required force creation being adequate to the object's mass value; b) the recognition of objects; c) robot control algorithm correction.

The idea of a trial motion regime comprises the process of an iterative increase in the compressive force value if the slippage signal is being detected. The continuous lifting regime provides the simultaneous object lifting process and increasing clamping force until the slippage signal disappears. The choice of the slip displacement data acquisition method depends on a robot's purpose,

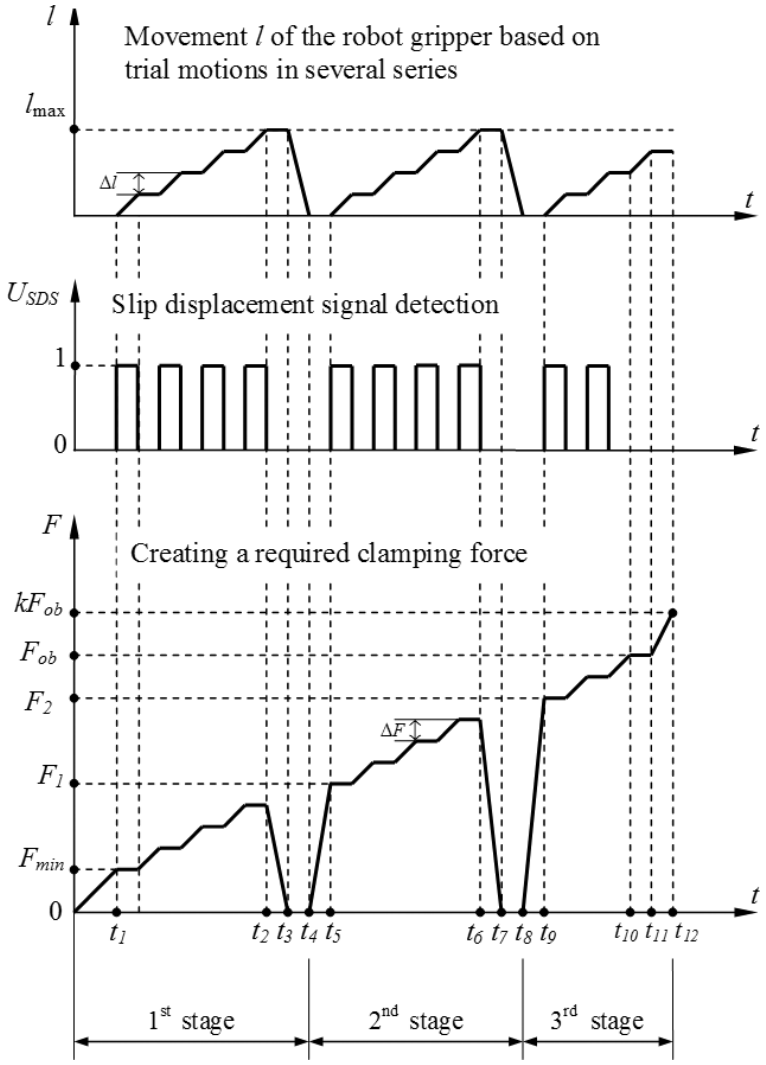

Figure 8.2 Series of trial motions with increasing clamping force F of gripper fingers based on object slippage.

the salient features of its functioning medium, the requirements of its response speed and the performance in terms of an error probability.

Figure 8.3 illustrates the main tasks in robotics which can be solved based on slip displacement signal detection.

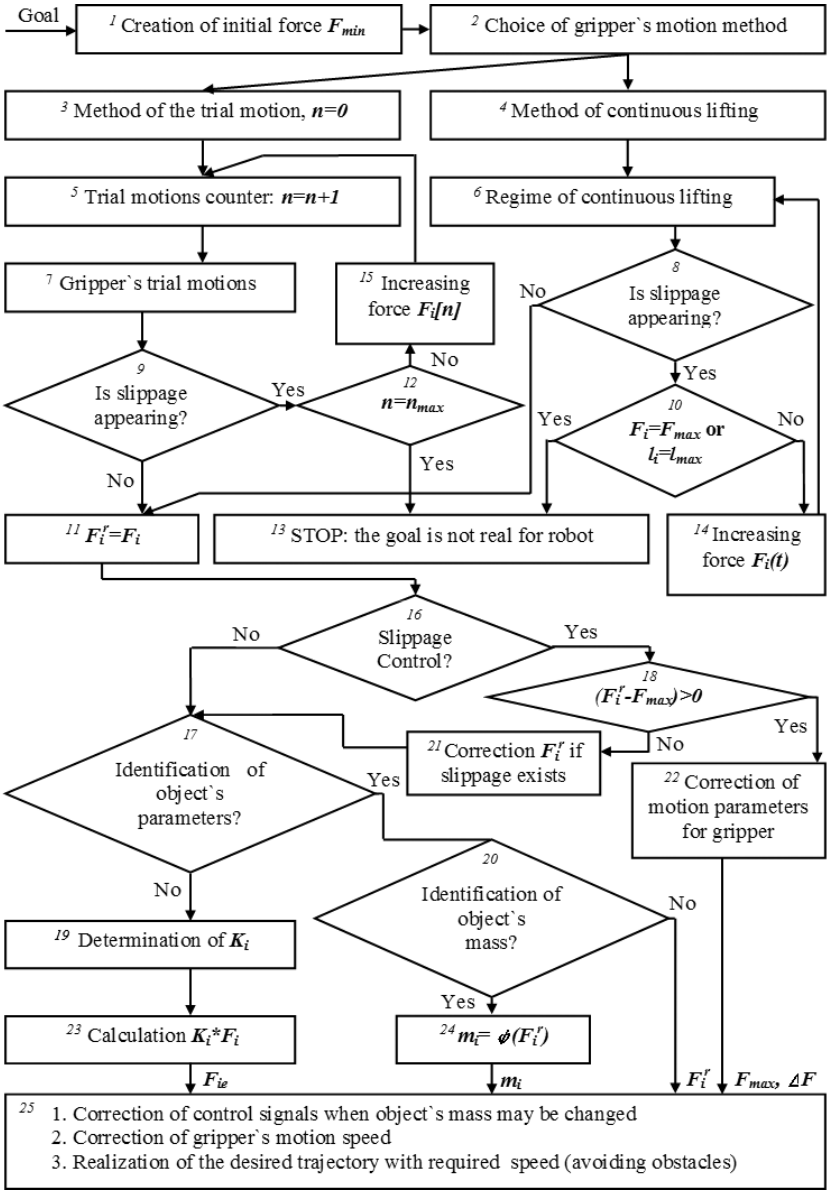

Figure 8.3 The algorithm for solving different robot tasks based on slip signal detection.

8.3 Analysis of Methods for Slip Displacement Sensors Design

Let's consider the main methods of slip displacement data acquisition, in particular [3, 4, 10, 11, 14, 17, 18, 20, 22]:

The vibration detection method. This method is based on a principle of the vibration detection in the sensing element when the object is slipping. To implement the method mentioned, the following sensing elements may be adopted: a sapphire needle interacting with the crystal receiver or a rod with a steel ball, connected to the electromagnetic vibrator.

The pressure re-distribution detection method. The method relies on the detection of a distribution change in pressure between gripper fingers at object slippage and is based on the physiological sensitivity function of human skin. The pressure transducers serve as nerves and are surrounded by an elastic substance as in the human body.

The rolling motion detection method. The method is characterized by transducing the object displacements in the vertical direction when slipping to the rolling motion of a sensitive element. A slip displacement signal is detected through rolling of a cylinder roller with elastic covering and a large friction coefficient. The roller's rolling motions may be converted into an electric signal by means of photoelectric or magnetic transducers, containing a permanent magnet on a movable roller, and in the case of a magnetic head being placed on a gripper.

The impact-sliding vibrations detection method. A core of the method implies the detection of liquid impact-sliding vibrations when the object is slipping. An acrylic disk with cylinder holes is used in the slip displacement sensor, realizing the method under consideration. A rubber gasket made in the form of a membrane protects one end of the disk, and a pressure gauge is installed on the other end. The hole is filled with water so that its pressure slightly exceeds the atmospheric pressure. While the motion of the object is in contact with a membrane, the impact-sliding vibrations are appearing and, therefore, inducing impulse changes on the water pressure imposed by a static pressure.

The acceleration detection method. This method is based on the measurement of accelerations of the sensing element motion by the absolute acceleration signal separation. The slip displacement sensor, comprising two accelerometers, can be used in this case. One of the accelerometers senses the absolute acceleration in the gripper, another responds to the acceleration of the sensitive plate springing when the detail is slipping. The sensor is attached to

the computer identifying the slip displacement signal by comparing the output signals of both accelerometers.

The interference pattern change detection method. This method involves the conversion of the intensity changes reflected from the moving surface of the interference pattern. The intensity variation of the interference pattern is converted to a numerical code, the auto-correlation function is computed and it achieves its peak at the slip displacement disappearance.

The configuration change detection in the sensitive elements method. The essence of the method incorporates the measurement of the varying parameters when the elastic sensitive element configuration changes. The sensitive elements made of conductive rubber afford coating of the object surface protruding above the gripper before the trial motion. When the object is displacing from the gripper, the configuration changes, the electrical resistance of such sensitive elements changes accordingly, confirming the existence of slippage.

The data acquisition by means of the photoelastic effect method. An instance representing this method may be illustrated by a transducer, in which, under the applied effort, the deformation of sensitive leather produces the appearance of voltage in the photoelastic system. The object slippage results in the change of the sensitive leather deformation being registered by the electronic visual system. The photosensitive transducer is a device for the transformation of interference patterns into the form of a numerical signal. The obtained image is of binary character, each pixel gives one bit of information. The binary representation of each pixel enables to reduce the processing time.

The data acquisition based on friction detection method. The method ensures the detection of the moment when the friction between the gripper fingers and the object to be grasped goes from friction at rest to dynamic friction.

Method of fixing the sensitive elements on the object. The method is based on fixing the sensitive elements on the surface of the manipulated objects before the trial motions with the subsequent monitoring of their displacement relative to the gripper at slipping.

Method based on recording oscillatory circuit parameters. The method is based on a change in the oscillatory circuit inductance while the object slips. The inductive slip sensor with a mobile core, stationary excitation winding and solenoid winding being one of the oscillatory circuit branches implements the method. The core may move due to the solenoid winding. The reduction of the solenoid winding voltage indicates the process of lowering. The core is lowering under its own weight from the gripper center onto the object

to be grasped. The oscillatory circuit induces the forced oscillations with the frequency coinciding with the frequency of excitation in the excitation winding.

The video signal detection method. The basis of this method constitutes a change in detection and ranging of patterns or video pictures as an indication of object slippage. The slip displacement detection is accomplished by means of the location sensors or visual sensors based on a laser source that has either a separated and reflecting beam or a vision with a non-coherent beam of light conductors for picture lighting and a coherent beam for image transmission.

The choice of a slip displacement detection method involves the multicriterion approach taking into account the complexity of implementation, the bounds of functional capabilities, mass values and overall dimensions, reliability and cost.

8.4 Mathematical Model of Magnetic Slip Displacement Sensor

8.4.1 SDS Based on "Permanent Magnet/Hall Sensor" Sensitive Element and Its Mathematical Model

In this chapter, the authors consider a few instances of updating the measurement systems. To suit the requirements of increasing the noise immunity of the vibration measurement method, a modified method has been developed. The modified method is founded on the measurement of the sensitive element angular deviation occurring at the object slippage (Figure 8.4).

Let's consider the structure and mathematical model (MM) of the SDS developed by the authors with a magnetic sensitive element which can detect the bar's angular deviation appearing at object slippage (Figure 8.4). The dependence $U = f(\alpha)$ can be used to determine the sensitivity of the SDS and the minimal possible amplitudes of the robot trial motions.

To construct the mathematical models, consider a magnetic system comprising a prismatic magnet with dimensions $c \times d \times l$, which is set to ferromagnetic plane with infinite permeability $\mu = \infty$ (Figure 8.5), where: c- width, d- length, and l- height of magnet, $(d >> l)$. The point $P(X_P, Y_P)$ is the observation point, which is located on the vertical axis and can change its position relative to the horizontal axis Ox or vertical axis Oy.

A Hall sensor with a linear static characteristic is located at the observation point P. Let's form the mathematical model for the determination of the magnetic induction B and the output voltage U_{out} (P) of the Hall sensor in

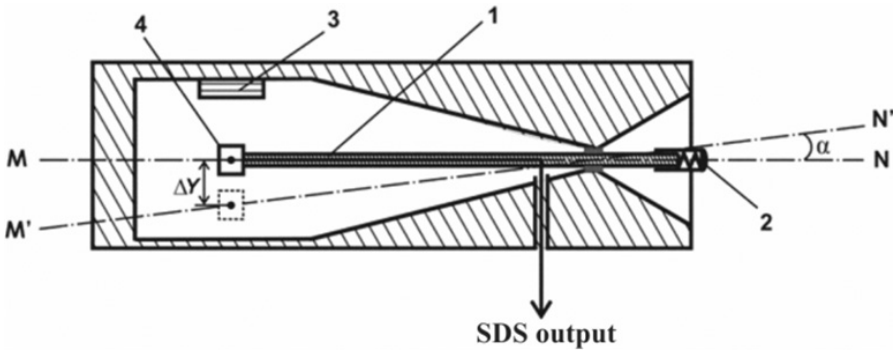

Figure 8.4 Magnetic SDS: 1– Rod; 2– Head; 3– Permanent magnet; 4– Hall sensor.

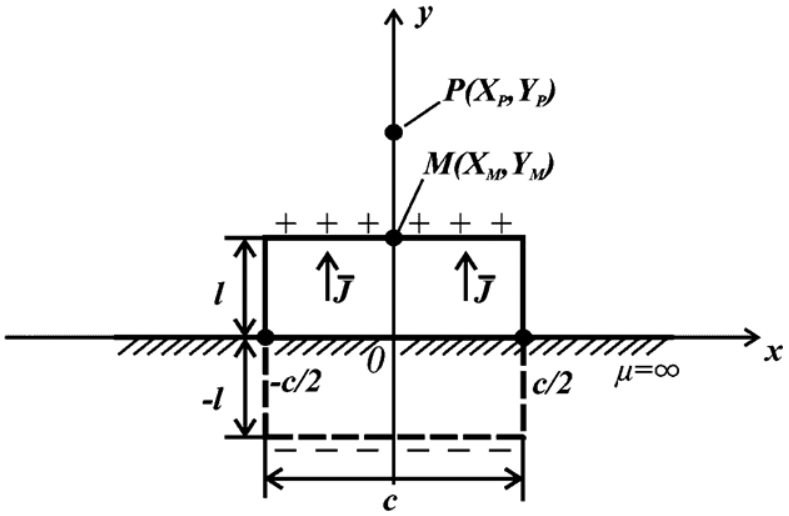

Figure 8.5 Model of magnetic sensitive element.

relation to an arbitrary position of the observation point P under the surface of the magnet.

The value of magnetic induction (outside the magnet volume) is $\bar{B} = \mu_0 \bar{H}$, where μ_0 is a magnetic constant; $\bar{H}$ is the magnetic field strength vector.

In the middle of the magnet– the magnetic induction value is determined by the dependence $\bar{B} = \mu_0(\bar{J} + \bar{H})$, where J is a magnetization value.

$$J = J_0 + \chi H,$$

where χ is a magnetic susceptibility; J_0 is the residual magnetization value.

The permanent magnet can be represented [26-28] as a simulation model of the surface magnetic charges that are evenly distributed across the magnet pole faces with the surface density J_T.

Thus, a y- component of the magnetic field strength H_y of the magnetic charges can be calculated as:

$$H_y = -\frac{J_T}{2\pi}\left[\left(\operatorname{arctg}\frac{X_p+c/2}{l-Y_p} - arctg\frac{X_p-c/2}{l-Y_p}\right) - \left(\operatorname{arctg}\frac{X_p+c/2}{-l-Y_p} - arctg\frac{X_p-c/2}{-l-Y_p}\right)\right], \tag{8.1}$$

and the y- component of magnetic induction B_y can be presented as:

$$B_y = -\frac{J_T\mu_0}{2\pi}\left[\left(\operatorname{arctg}\frac{X_p+c/2}{l-Y_p} - arctg\frac{X_p-c/2}{l-Y_p}\right) - \left(\operatorname{arctg}\frac{X_p+c/2}{-l-Y_p} - arctg\frac{X_p-c/2}{-l-Y_p}\right)\right],$$

To determine the parameter J_T, it is necessary to measure the induction of the pole faces center $B_y\Big|_{x=0,y=l+}$. Value ($y = l+$) indicates that the measurement of B_{mes} is conducted outside the volume of the magnet. The value of magnetic induction at a point with the same coordinates on the inside of the pole faces can be considered equal to the value of induction from the outside pole faces by virtue of the continuity of the magnetic flux and lines of magnetic induction, namely:

$$B_y\Big|_{x=0,y=l+} = B_y\Big|_{x=0,y=l-}.$$

So, we can write: $B_y\Big|_{x=0,\,y=l+} = B_{mes} = \mu_0 J_t + \mu_0 H_y\Big|_{x=0,y=l-}$, where B_{mes} is the value of magnetic induction measured at the geometric center of the top pole faces of the prismatic magnet.

On the basis of (8.1), we obtain:

$$B_{mes} = \mu_0 J_T\left[1 - \lim_{(Yp\to l-)}\frac{2}{2\pi}\left(arctg\frac{c/2}{l-Y_p} + arctg\frac{c/2}{l+Y_p}\right)\right]$$

$$= \mu_0 J_T\left(\frac{1}{2} + \frac{1}{\pi}arctg\frac{c}{4l}\right),$$

$$J_T = \frac{2\pi B_{mes}}{\mu_0\left(\pi + 2arctg\frac{c}{4l}\right)}.$$

For the *y*- component of the magnetic induction B_y **(***P***)** at the observation point *P,* the following expression was obtained:

$$B_y(p) = -\frac{B_{mes}}{\left(\pi + 2arctg\frac{c}{4l}\right)}\left[\left(arctg\frac{X_p + c/2}{l - \mathrm{Y}_p} - arctg\frac{X_p - c/2}{l - \mathrm{Y}_p}\right) - \left(arctg\frac{X_p + c/2}{-l - \mathrm{Y}_p} - arctg\frac{X_p - c/2}{-l - \mathrm{Y}_p}\right)\right]. \quad (8.2)$$

8.4.2 Simulation Results

For the analysis of the existing mathematical model (8.2), let's calculate the value of magnetic induction on the surface of the magnet (Barium Ferrite) with parameters of c=0.02m, d=0.08m, l=0.014m and a value of magnetic induction B_{mes} = 40 mT (value measured at the geometric center of the upper limit of the magnet).

The simulation results for the magnetic induction are represented as $B_y = f_i(X_P), i$ = 1,2,3 above the magnet for different values of the height Y_P of the observation point $P\,(X_P, Y_P)$, where indicated:

$f_1 - for$ $\quad B_y\Big|_{x\in[-20;20]mm, y=l+1mm}$;

$f_2 - for$ $\quad B_y\Big|_{x\in[-20;20]mm, y=l+5mm}$;

$f_3 - for$ $\quad B_y\Big|_{x\in[-20;20]mm, y=l+20mm}$.

As can be seen from Figure 8.6, the magnetic induction $B_y = f_1\ (X_P)$ above the surface of the magnet is practically constant for the coordinate $X_P \in$ [–5; 5] mm, which is half of the corresponding size of the magnet. If the distance between the observation point *P* and magnet increases ($f_2\ (X_P)$, $f_3\ (X_P)$ in Figure 8.6), the curve shape changes become more gentle, with a pronounced peak above the geometric center of the top pole faces of the prismatic magnet (at the point X_P = 0).

For the Hall sensor (Figure 8.4) in the general case, the dependence of the output voltage U_{out} (*P*) on the magnitude of the magnetic induction B_y is defined as:

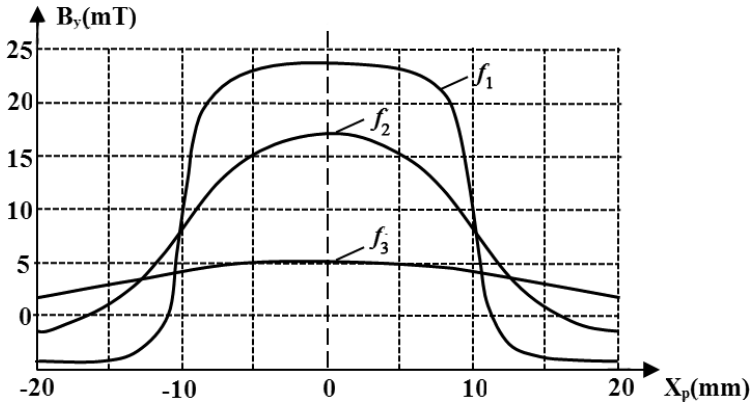

Figure 8.6 Simulation results for B_y (*P*) based on the mathematical model (8.2).

$$U_{out}\ (P) = U_c + kB_y(P), \tag{8.3}$$

where k is the correction factor, that depends on the type of Hall sensor; U_c is a constant component of the Hall sensor output voltage.

For Hall sensors with linear dependence of the output signal U_{out} on the magnetic induction B_y, $k = const$ and $k = f\{B_y\ (P)\}$ for nonlinear dependence (8.3). For Hall sensor SS490 (Honeywell) with linear dependence (8.3), the values of the parameters are: $U_c = 2.5V$ and $k = 0.032$ (according to the static characteristic of the Hall sensor). The authors present the mathematical model of the Hall sensor output voltage $U_{out}\ (Y_P)$ at its vertical displacement above the geometric center of the top pole faces of magnet $(X_P = 0)$:

$$U_{out}(Y_P) = 2,5 + 7,4 \times 10^{-3} \left(arctg \frac{0,01}{0,014 - Y_P} + arctg \frac{0,01}{0,014 + Y_P} \right). \tag{8.4}$$

The comparative results for dependences $U_{out}\ (Y_p)$, $U_E\ (Y_p)$ and $U_R(Y_p)$ are presented in Figure 8.7, where $U_{out}\ (Y_p)$ was calculated using MM (8.4), $U_E\ (Y_p)$ are the experimental results according to [7] and $U_R\ (Y_p)$ is a nonlinear regressive model according to [8].

The comparative analysis (Figure 8.7) of the developed mathematical model $U_{out}\ (Y_p)$ with the experimental results $U_E\ (Y_p)$ confirms the correctness and adequacy of the synthesized models (8.1)–(8.4).

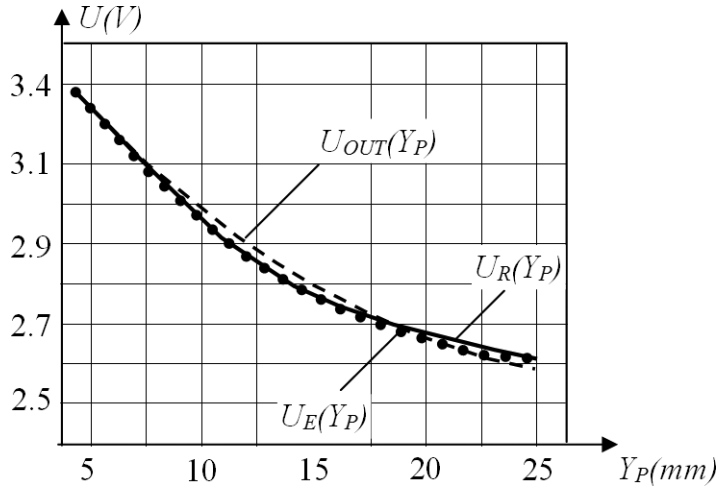

Figure 8.7 Comparative analysis of modeling and experimental results.

8.5 Advanced Approaches for Increasing the Efficiency of Slip Displacement Sensors

This study presents a number of sensors for data acquisition in real time [5, 11, 13, 14]. The need for rigid gripper orientation before a trial motion has caused the development of the slip sensor based on a cylinder roller with a load which has two degrees of freedom [3, 14].

The sensitive element of the new sensor developed by the authors has the form of a ball (Figure 8.8) with light-reflecting sections disposed in a staggered order (Figure 8.9), thus providing slippage detection by the photo-method.

The ball is arranged in the sensor's space through spring-loaded slides. Each slide is connected to the surface of the gripper's space by an elastic element made of conductive rubber.

The ball motion is secured by friction-wheels and is measured with the aid of incremental transducers in another modification of the slip sensor with the ball acting as a sensitive element. The ball contacts with the object through the hole. In this case, the ball is located in the space of compressed air dispensed through the hole.

For the detection of the sensitive element angular deviation during object slippage in any direction, the authors propose [12] a slip displacement sensor with a measurement of changeable capacitance (Figure 8.10).

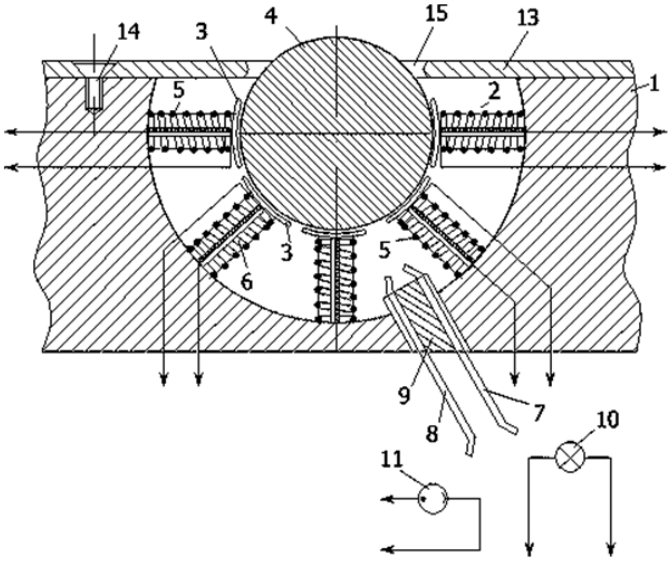

Figure 8.8 The ball as sensitive element of SDS: 1– Finger of robot's gripper; 2– Cavity for SDS instalation; 3– Guides; 4– Sensitive element (*a* ball); 5– Spring; 6– Conductive rubber; 7, 8– Fiber optic light guides; 9– *a* Sleeve; 10– Light; 11– Photodetector; 13–Cover; 14–Screw; 15–Hole.

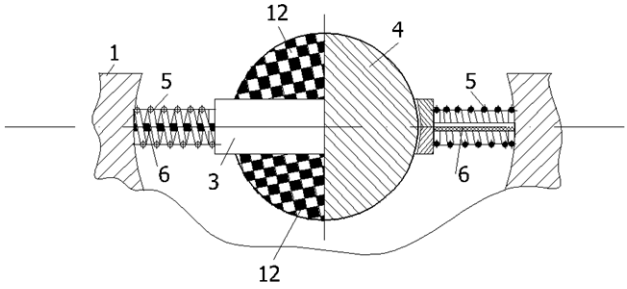

Figure 8.9 Light-reflecting surface of the sensitive ball with reflecting and absorbing portions (12) for light signal.

The structure of the intelligent sensor system developed by the authors which can detect the direction of object slippage based on the capacitated SDS (Figure 8.10) is represented in Figure 8.11 with channels of information processing and electronic units that implement the intellectual base of production rules to identify the direction of displacement of the object in the gripper (if there is a collision with an obstacle).

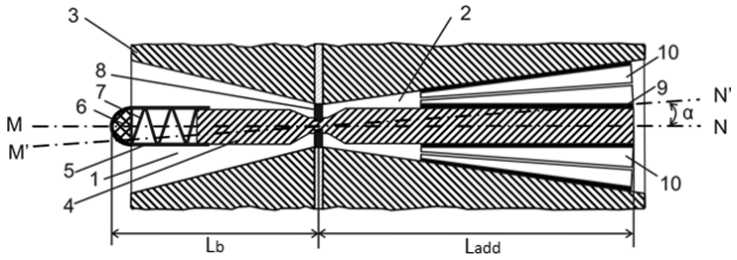

Figure 8.10 Capacitated SDS for the detection of object slippage in different directions: 1– Main cavity of robot's gripper; 2– Additional cavity; 3– Gripper's finger; 4– Rod; 5– Tip; 6– Elastic working surface; 7– Spring; 8– Resilient element; 9, 10– Capacitor plates.

The SDS is placed on at least one of the gripper fingers (Figure 8.10). The recording element consists of four capacitors distributed across the conical surface of the additional cavity (2). One plate (9) of each capacitor is located on the surface of the rod (4) and the second plate (10) is placed on the inner surface of the cavity (2).

The intelligent sensor system (Figure 8.11) provides an identification of signals corresponding to object slippage direction $\{N, NE, E, SE, S, SW, W, NW\}$ in the gripper in the cases of contacting obstacles.

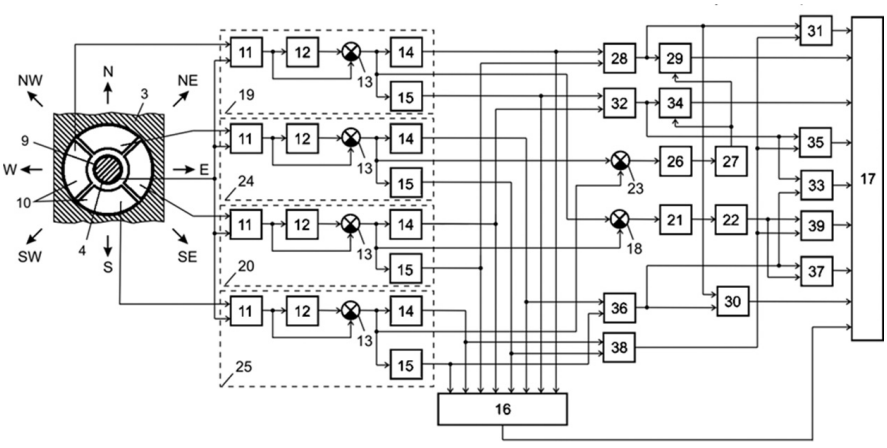

Figure 8.11 Intelligent sensor system for identification of object slippage direction: 3– Gripper's finger; 4– Rod; 9, 10– Capacitor plates; 11– Converter "capacitance-voltage"; 12– Delay element; 13, 18, 23– Adders; 14, 15, 21, 26– Threshold elements; 16– Multi-Inputs element OR; 17– Computer information-control system; 19, 20, 24, 25– Channels for sensor information processing; 22, 27– Elements NOT; 28–39– Elements AND.

The implementation of relation (Figure 8.10)

$$\frac{L_b}{L_{add}} = \frac{1}{5}$$

allows to increase the sensitivity of developed sensor system.

Initially (Figure 8.10), the tip (5) is held above the surface of the gripper's finger (3) by a spring (7), and a resilient element (8) holds a rod (4) in such a position that its longitudinal axis is perpendicular to the surface of the finger and coincides with the axis MN of the rod (4). When gripping a manipulation object, its surface comes in contact with the tip (5), the spring (7) is compressed and the tip (5) is immersed in a cavity (2). At this moment, the value of compressive force corresponds to the minimal pre-determined value F_{min} that eliminates distortion or damage of the object.

The object begins to slip in the gripper if an inequality between compressive force and the mass of the object exists during the trial motion. In this case, the rod (4) is deflecting along the sliding direction on the angle α as the result of the friction forces between the object's contacting surface and the working surface (6) of the tip (5).

Thus, the longitudinal axis of the rod (4) coincides with the axis M′N′. Reciprocal movement of plates (9) and (10) with respect to each other in all capacitative elements leads to value changes of the capacities C_1, C_2, C_3 and C_4 depending on the direction of rod's movement. The changes of the capacities lead to the voltage changes at the outputs of the respective convertors "capacitance-voltage" in all sensory processing channels.

From time to time, the robot's gripper may be faced with an obstacle when the robot moves a manipulation object in dynamic environments according to preplanned trajectories. The obstacles can appear randomly in the dynamic working area of the intelligent robot. As a result of the collision between the robot gripper and the obstacle, object's slippage may appear if the clamping force F is not enough for reliable fixation of object between the gripper's fingers. The direction {*N, NE, E, SE, S, SW, W, NW*} of such slip displacement of the object depends on the position of the obstacle in the desired trajectory.

In this case, the output signal of element OR (16) is equal to 1 and this is a command signal for the computer system (17) which constrains the implementation of the planned trajectory. At the same time, the logical 1 signal appears at the output of one of the AND elements {29, 30, 31, 33, 34, 35, 37, 39} that corresponds to one of the object's slippage direction {*N, NE, E, SE, S, SW, W, NW*} in the robot gripper.

Let's consider, for example, the determination of slippage direction $\{N\}$ after the contact between the obstacle and robot gripper (with object). If the object slips in direction $\{N\}$ (Figure 8.11), then:

- the capacity C_1 in first channel (19) increases and a logical 1 signal appears at the output of threshold element (14) and at the first input of the AND element (28);
- the capacity C_3 in the third channel (20) decreases and a logical 1 signal appears at the output of threshold element (15), at the second input and output of AND element (28) and at the first input of the AND element (29);
- the capacities C_2, C_4 of the second (24) and fourth (25) channels of the sensor information processing are equivalent $C_2 = C_4$ and in this case a logical 0 signal appears at the outputs of adder (23) and threshold element (26), a logical 1 signal appears at the output of NOT element (27), at the second input and output of AND element (29) and at the second input of the computer information-control system (17). It means that the direction of the object's slippage is $\{N\}$, taking into account that output signals of the AND elements $\{30, 31, 33, 34, 35, 37, 39\}$ equal 0.

The production rules "IF-THEN" base are represented in Table 8.1. This rule base determines the functional dependence between the direction of object slippage (Figure 8.11), the current state of each capacitor $\{C_1, C_2, C_3, C_4\}$ and the corresponding output signals $\{U_1, U_2, U_3, U_4\}$ of the multi-capacitor slip displacement sensor, where: U_i, (i = 1...4)– output signal of i-th converter "capacitance - voltage" (11); (>)– indicator of the corresponding signal U_i,(i = 1...4) increases during the object slippage process; (<)– indicator of the corresponding signal U_i,(i = 1...4) decreases during the object slippage process; (=)– pair's indicator of equivalence according to

Table 8.1 The base of production rules "IF-THEN" for indetification of the slip displacement direction

Number of	Antecedent				Consequent
Production Rule	U_1	U_2	U_3	U_4	Direction of Slippage
1	>	=	<	=	*N*
2	>	>	<	<	*NE*
3	=	>	=	<	*E*
4	<	>	>	<	*SE*
5	<	=	>	=	*S*
6	<	<	>	>	*SW*
7	=	<	=	>	*W*
8	>	<	<	>	*NW*

conditions $U_i = U_j$, (i = 1...4), (j = 1...4), $i \neq j$ in the antecedents of the production rules.

The mathematical models of different types of slip displacement sensors with a measurement of changeable capacity are presented in [5, 19, 21, 23].

8.6 Advances in Development of Smart Grippers for Intelligent Robots

8.6.1 Self-Clamping Grippers of Intelligent Robots

The slip displacement signals, which are responsible for the creation of the required compressive force adequate to the object mass, provide the conditions for the correction of the gripper trajectory-planning algorithm, which identifies an object mass as a variable parameter [9]. The object mass identification is carried out in response to the final value of the compressive force, recorded at the slippage signal disappearance. It is of extreme importance to employ slip sensors with uprated response when the object mass changes in the functioning process.

In those cases when the main task of the sensing system is the compression of the object without its deformation or damage, it is expedient in future research to project the advanced grippers of a self-clamping design (Figure 8.12), excluding the gripper drive for the compressive force growth (at slippage) up to the required value.

The information processing system of a self-adjusting gripper of an intelligent robot with angle movement of clamping rollers consists of: 24– control unit; 25– delay element; 26, 30, 36– adder; 27, 32, 37, 41– threshold element; 28, 29, 31, 33, 34, 35, 38, 40, 42– switch; 39– voltage source.

In such a gripper (Figure 8.12), the rollers have two degrees of freedom and during object slippage they have a compound behavior (rotation and translation motions). This gripper (Figure 8.12) is adaptive since object self-clamping is being accomplished with a force adequate to the object mass up to the moment of the slippage disappearance [6, 14].

Another example of a developed self-clamping gripper [15] is represented in Figure 8.13, where: 1– finger; 2– roller axis; 3– roller; 4– sector element; 5– guide gear racks; 6– pinion; 7– travel bar; 8, 9– axis; 10– object; 11– elastic working surface; 12, 13– spring; 14, 15– clamping force sensor; 16– electroconductive contacts; 17, 18– fixator; 19, 20– pintle.

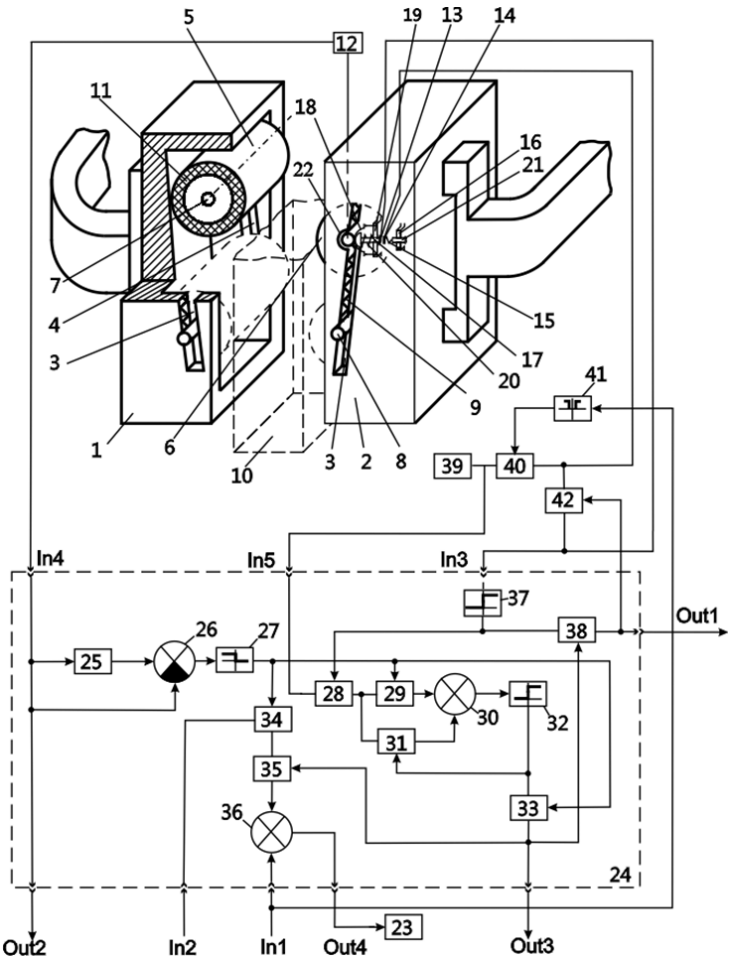

Figure 8.12 Self-adjusting gripper of an intelligent robot with angle movement of clamping rollers: 1, 2– Finger; 3, 4– Guide groove; 5, 6– Roller; 7, 8– Roller axis; 9, 15, 20– Spring; 10– Object; 11, 18– Elastic working surface; 12– Clamping force sensor; 13, 14– Electroconductive contacts; 16, 19– Fixator; 17– Stock; 21– Adjusting screw; 22– Deepening; 23– Finger's drive.

The experimental self-clamping gripper with plane-parallel displacement of the clamping rollers and intelligent robot with 4 degrees of freedom for experimental investigations of the developed grippers and slip displacement sensors are represented in Figure 8.14 and Figure 8.15, correspondingly.

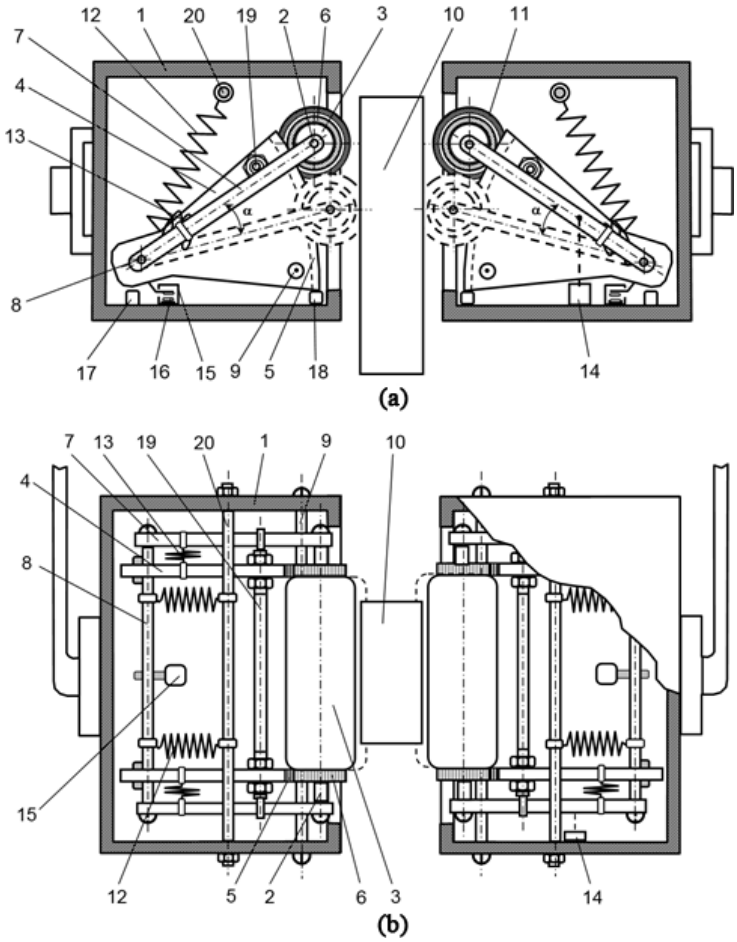

Figure 8.13 Self-clamping gripper of an intelligent robot with plane-parallel displacement of the clamping roller: Front view (a); Top view (b).

8.6.2 Slip Displacement Signal Processing in Real Time

Frequent handling operations require a compressive force being exerted through the intermediary of the robot's sensing system in the continuous hoisting operation. This regime shows a simultaneous increase in the compressive force while the continuous hoisting operation and lifting of the gripper in the vertical direction take place accompanied by the slip displacement signal measurement. When the slippage signal disappears, the compressive force does not increase and, therefore, the operations with the object are

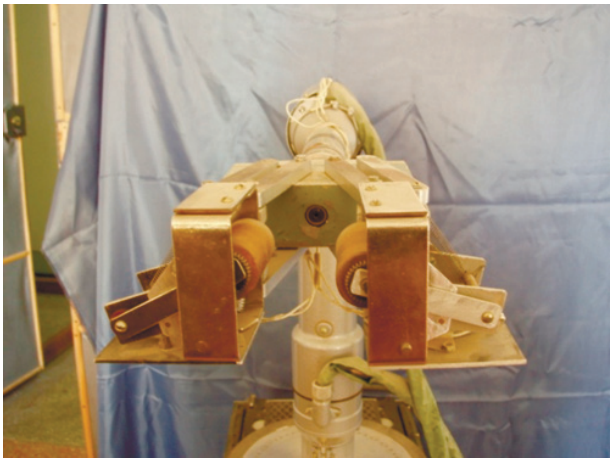

Figure 8.14 Experimental self-clamping gripper with plane-parallel displacement of the clamping rollers.

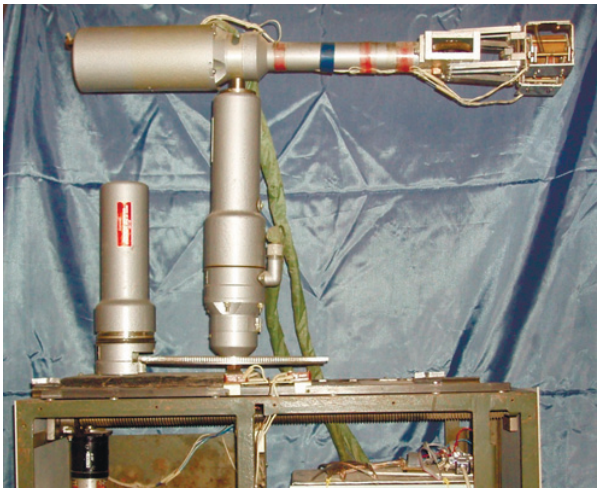

Figure 8.15 Intelligent robot with 4 degrees of freedom for experemental investigations of SDS.

accomplished according to the robot's operational algorithm. To realize the trial motion regime and the continuous hoisting operation being controlled in real time, stringent requirements to the parameters should be met, in particular:

- the response time between the moment of slippage emergence and the moment when the gripper fingers begin to increase the compressive force;

- the time of the sliding process including the moments between the emergence of sliding and its disappearance;
- the minimal object displacement detected by the slip signal.

The problem of raising the sensors response in measuring the slip displacement signals is tackled by improving their configuration and using the measuring circuit designs with high resolving power.

8.7 Conclusions

The slip displacement signal detection method considered in the present paper furnishes an explanation of the main detection principles and allows robot sensing systems to obtain broad capabilities. The authors developed a wide variety of SDS schemes and mathematical models for capacitative, magnetic and light-reflecting sensitive elements with improved characteristics (accuracy time response, sensitivity). It is very important that the developed multi-component capacity sensor allows identifying the direction of object slippage based on slip displacement signal detection which can appear in the case of intelligent robot collisions with any obstacle in a dynamic environment. The design of self-clamping grippers is also a very appropriate direction for intelligent robot development.

The results of the research are applicable in the automatic adjustment of the clamping force of robot's gripper and robot motion correction algorithms in real time. The methods introduced by the authors may be also used in random operational conditions, within problems of automatic assembly, sorting, pattern and image recognition in the working zones of robots. The proposed sensors and models can be used for the synthesis of intelligent robot control systems [2, 16] with new features and for solving orientation and control tasks during intelligent robot contacts with obstacles.

References

[1] Ravinder S. Dahiya, Giorgio Metta, Maurizio Valle and Giulio Sandini. Tactile Sensing From Humans to Humanoids, volume 26 of Issue 1, pages 1–20. IEEE Transactions on Robotics, 2010.

[2] A. A. Kargin. Introduction to Intelligent Machines. Book 1: Intelligent Regulators. Nord-Press, DonNU, Donetsk, 2010.

[3] Y. P. Kondratenko. Measurements methods for slip displacement signal registration. In Proc. of Intern. Symposium on Measurement Technology and Intelligent Instruments, pages 1451–1461, Chongqing-Wuhan, China, 1993. Published by SPIE. USA.

[4] Y. P. Kondratenko and X. Y. Huang. Slip displacement sensors of robotic assembly system. In Proc. of 10-th Intern. Conference on Assembly Automation, pages 429–436, Kanazava, Japan, 23–25 Oct 1989. IFS Publications. Kempston, United Kingdom.

[5] Y. P. Kondratenko and I. L. Nazarova. Mathematical model of capacity sensor with conical configuration of sensitive element. In Proceedings of the Donetsk National Technical University, No. 11(186), pages 186–191, Donetsk: DNTU.

[6] Y. P. Kondratenko and E. A. Shvets. Adaptive gripper of intelligent robot. Patent No. 14569, Ukraine, 2006.

[7] Y. P. Kondratenko and O. S. Shyshkin. Experimental studies of the magnetic slip displacement sensors for adaptive robotic systems. In Proceedings of the Odessa Polytechnic University, pages 47–51, Odessa, 2005. Special Issue.

[8] Y. P. Kondratenko and O. S. Shyshkin. Synthesis of regression models of magnetic systems of slip displacement sensors. Radioelectronic and Computer Systems, (No. 6(25)): 210–215, Kharkov, 2007.

[9] Y. P. Kondratenko, A. V. Kuzmichev and Y. Z. Yang. Robot control system using slip displacement signal for algoritm correction. In ROBOT CONTROL (SYROCO91). Selected papers from the 3-rd IFAC/IFIP/IMACS Symposium, pages 463–469. Pergamon Press, Vienna, Austria. Oxford-NewYork-Seoul-Tokyo, 1991.

[10] Y. P. Kondratenko, E. A. Shvets and O. S. Shyshkin. Modern sensor systems of intelligent robots based on the slip displacement signal detection. In Annals of DAAAM for 2007 & Proceedings of the 18th International DAAAM Symposium, pages 381–382, Vienna, Austria, 2007. DAAAM International.

[11] Y. P. Kondratenko, L. P. Klymenko, V. Y. Kondratenko, G. V. Kondratenko and E. A. Shvets. Slip displacement sensors for intelligent robots: Solutions and models. In Proceedings of the 2013 IEEE 7th International Conference on Intelligent Data Acquisition and Advanced Computing Systems, Vol. 2, pages 861–866. IDAACS, 2013.

[12] Y. P. Kondratenko, N. Y. Kondratenko and V. Y. Kondratenko. Intelligent sensor system. Patent No. 52080, Ukraine, 2010.

[13] Y. P. Kondratenko, O. S. Shyshkin and V. Y. Kondratenko. Device for detection of slip displacement signal. Patent No. 79155, Ukraine, 2007.

[14] Y. P. Kondratenko, V. Y. Kondratenko, E. A. Shvets and O. S. Shyshkin. Adaptive gripper devices for robotic systems. In Mechatronics and Robotics (M&R-2007): Proceeding of Intern. Scientific-and-Technological Congress (October 2–5, 2007), pages 99–105. Polytechnical University Press, Saint-Petersburg, 2008.

[15] Y. P. Kondratenko, V. Y. Kondratenko, I. V. Markovsky, S. K. Chernov, E. A. Shvets and O. S. Shyshkin. Adaptive gripper of intelligent robot. Patent No. 26252, Ukraine, 2007.

[16] Y. P. Kondratenko, Y. M. Zaporozhets, G. V. Kondratenko and O. S. Shyshkin. Device for identification and analysis of tactile signals for information-control system of the adaptive robot. Patent No. 40710, Ukraine, 2009.

[17] M. H. Lee. Tactile sensing: New directions, new challenges. Int. J. of Robotics Research. 19(7), Jul 2000, vol. 19 no. 7, pp. 636–643., Jul 2000.

[18] Mark H. Lee and Howard R. Nicholls. Tactile sensing for mechatronics - a state of the art survey, volume 9, pages 1–31. Mechatronics, 1999.

[19] H. B. Muhammad, C. M. Oddo, L. Beccai, C. Recchiuto, C. J. Anthony, M. J. Adams, M. C. Carrozza, D. W. L. Hukins and M. C. L. Ward. Development of a bioinspired MEMS based capacitive tactile sensor for a robotic finger. Sensors and Actuators A-165, pages 221–229, 2011.

[20] Howard R. Nicholls and Mark H. Lee. A survey of Robot Tactile Sensor Technology. The International Journal of Robotic Research, (Vol. 8, No. 3):3–30, June 1989.

[21] E. P. Reidemeister and L. K. Johnson. Capacitive acceleration sensor for vehicle applications. In Sensors and actuators, pages 29–34. SP-1066, 1995.

[22] Johan Tegin and Jan Wikander. Tactile Sensing in Intelligent Robotic Manipulation-A Review. Industrial Robot: An International Journal, (Vol. 32, No. 1):64–70, 2005.

[23] M. I. Tiwana, A. Shashank, S. J. Redmond and N. H. Lovell. Characterization of a capacitive tactile shear sensor for application in robotic and upper limb prostheses. Sensors and actuators, A-165, pages 164–172, 2011.

[24] M. Ueda and K. Iwata. Adaptive grasping operation of an industrial robot. In Proc. of the 3-rd Int. Symp. Ind. Robots, pages 301–310, Zurich, 1973.

[25] M. Ueda, K. Iwata and H. Shingu. Tactile sensors for an industrial robot to detect a slip. In 2-nd Int. Symp. on Industrial Robots, pages 63–76, Chicago, USA, 1972.

[26] Y. M. Zaporozhets. Qualitative analysis of the characteristics of direct permanent magnets in magnetic systems with a gap. Technical electrodynamics, (No. 3):19–24, 1980.

[27] Y. M. Zaporozhets, Y. P. Kondratenko and O. S. Shyshkin. Three-dimensional mathematical model for calculating the magnetic induction in magnetic-sensitive system of slip displacement sensor. Technical electrodynamics, (No. 5):76–79, 2008.

[28] Y. M. Zaporozhets, Y. P. Kondratenko and O. S. Shyshkin. Mathematical model of slip displacement sensor with registration of transversal constituents of magnetic field of sensing element. Technical electrodynamics, (No. 4):67–72, 2012.